Assessment of the photoprotective potential and structural characterization of secondary metabolites of Antarctic fungus Arthrinium sp

Ana Carolina Jordão
University of São Paulo
Gustavo Souza Santos
State University of Bahia
Thaiz Rodrigues Teixeira
University of São Paulo
Ana Júlia Pasuch Gluzezak
University of São Paulo
Clarissa Bechuate Souza Azevedo
University of São Paulo
Karina Castro Pereira
University of São Paulo
Ludmilla Tonani
University of São Paulo
Lorena Rigo Gaspar
University of São Paulo
Márcia Regina Von Zeska Kress
University of São Paulo
Pio Colepicolo
University of São Paulo
Hosana Maria Debonsi (hosana@fcfrp.usp.br)
University of São Paulo

Research Article

Keywords: Arthrinium, Marine Antarctic natural products, Photoprotection, Antioxidant, Reconstructed human skin

Posted Date: September 19th, 2023

DOI: https://doi.org/10.21203/rs.3.rs-3352625/v1

Additional Declarations: No competing interests reported.

Version of Record: A version of this preprint was published at Archives of Microbiology on December 23rd, 2023. See the published version at https://doi.org/10.1007/s00203-023-03756-w.

Abstract

Interest in Antarctic fungi has been growing due to their ability to survive in the harsh environment, suggesting the presence of compounds for human use. Due to the damaging effects of sunlight, sunscreen use has been growing but, scientific evidence has pointed to the toxic potential of UV filters for human and environment, leading to a ban the use of UV filters (avobenzone and oxybenzone) in some locations. So, this work evaluated the photoprotective potential of molecules from sustainable marine sources (seaweed-derived fungi), aiming to discover natural, efficient, and safer UV filter alternatives. Thus, photoprotective and antioxidant activity of metabolites from Arthrinium sp. was investigated. Six compounds (1-6) were isolated: 3-Hydroxybenzyl alcohol (1), (-)-orthosporin (2), norlichexanthone (3), anomalin B (4), anomalin A (5) and agonodepside B (6), being 1, 2, 6 not reported in Arthrinium. Fraction F showed excellent absorbance in both UVA and UVB, while compound 6 presented lower absorbance in the UVB region. Fraction F and compound 6 were considered photostable and non-phototoxic on HaCaT cells. Both showed antioxidant activity against UVA induced intracellular ROS production, in keratinocyte monolayers and in reconstructed human skin models (reduction of 34.6% and 30.2% in fluorescence) and both can be considered for use in sunscreens. Fraction F presented higher absorption in UVB and UVA than (6), which can be due to synergism and did not present any irritation potential in HET-CAM assay. The fraction presented the advantage of not needing further purifications, however clinical studies should be performed to confirm its potential.

Introduction

The marine environment is characterized by strong fluctuations in abiotic and biotic conditions such as high pressures, salinity, tides, depth and temperatures, for example. As a result, wide biological diversities and unique chemical compounds have emerged, making the marine environment an important source of new bioactive compounds with biotechnological applications. In addition, in the marine environment there is the presence of sessile living organisms, such as sponges, cnidarians, and algae, which have developed chemical defense mechanisms (Li et al., 2020). Surrounded by the Southern Ocean, the Antarctic continent is one of the most primitive and harsh ecosystems on the planet. This is due to low temperatures, low levels of organic nutrients, low water availability, strong winds, and high incidence of UV rays. However, even under these conditions, benthic algal communities, microorganisms thrive. Numerous species of fungi have been described in association with seaweeds in parasitic, saprophytic, or endophytic relationships. These organisms are collectively known as "algicolous fungi" and are relatively unexplored but hold great metabolic potential. Interest in Antarctic fungi, in particular, has been growing due to their ability to survive in the harsh Antarctic environment, which suggests the presence of unusual and promising biosynthetic pathways that could lead to novel bioactive compounds (Ogaki et al., 2019). These novel active compounds are targeted for application with different approaches, including insecticides, biotechnological insights and finally new cosmetic ingredients. Among the cosmetic application, is it possible to point sunscreens formulation, based on mycosporine-like amino acids (MAAs) contents, that are capable of absorbing the UV rays ranging from 310 to 360 nm. MAAs are colorless, soluble in water and have low molecular weight which can be found in fungi, algae, cyanobacteria, among other marine organisms (Rosic, 2021; Ding et al., 2022). Furthermore, some other natural compounds were reported as having anti-UV activity, such as the phenolic substances. In nature, phenolic compounds are biosynthesized to balance ROS production and present protective effects against DNA damage induced by UV radiation (Bedoux et al., 2014; Ding et al., 2022). Agonodepside B (compound **6**) is a depside, a natural product class commonly formed by two or more phenolic

units, biosynthetically originated from the polyketide synthase (PKS) route (Kealey et al., 2021; Legaz et al., 2011).

It is well-known that chronic exposure to UV radiation from sunlight has negative health effects, and a growing concern about such effects has caused an increase in the use of formulations containing UV filters (Watkins et al., 2021). In addition to sunscreens, these substances are used in more than 2.000 personal cosmetic products (Dinardo and Downs, 2018; Zhang et al., 2021). The global production of UV filters is estimated to be more than 10.000 tons per year. Inevitably, these products end up being released into the aquatic environment, either directly, such as by swimming in this environment; or indirectly, such as by washing the product off while bathing. This release is increasing concerns about the impact of the presence of these substances in the aquatic environment (Zhang et al., 2021). *In vivo* and *in vitro* studies show vast adverse effects caused to the environment and exposed organisms, such as coral reef bleaching and toxicity to the endocrine, neurological, and other systems of resident organisms (Fivenson et al., 2020). In response to these studies concerning environment injury, some regions have banned the use of some UV filters, such as oxybenzone (benzophenone-3) and octinoxate (ethylhexyl methoxycinnamate). These bans take place in Hawaii, the US Virgin Islands, Key West in Florida, Palau, and Bonaire (Mitchelmore et al., 2021).

There is a need, therefore, for eco-friendly, sustainable and safer UV filters as alternatives to the synthetic compounds available in the cosmetic market (Fivenson et al., 2020). Several organisms, especially those exposed to intense UV radiation, have developed various photo adaptive mechanisms including production of antioxidants and UV absorbing metabolites (Saewan and Jimtaisong, 2015). UV incidence is also highly evident in the Antarctic region. Despite the decrease of ozone-depleting compounds and its consequent recovery, the Antarctic ozone hole continues to occur each year, with the severity of ozone loss strongly modulated by weather conditions, persisting mainly in late spring (Cordero et al. 2022).

Thus, the search for safer, effective and less environmentally aggressive UV filters produced by organisms of Antarctic origin is promising and justified.

Material and Methods

Fungal Isolation

Initially, a health specimen of the seaweed *Phaeurus antarcticus* was collected at Greenwich Island, Antarctica (62°26’46.9” S 59°44’20.3” W) in November/2015 during the Brazilian Antarctic Expedition OPERANTAR XXXIII. The seaweed was rinsed in sterile seawater to remove adherent debris and other contaminants. To the selective isolation of fungal endophytes, the seaweed was cut into small fragments (0,5 – 1,5 cm) and surface disinfected by immersion in 70% ethanol (v/v) for 15 seconds, followed by rinsing in sterile seawater three times. Control plates were used to assess the efficiency of the disinfection procedure. The disinfected fragments were used to make imprints on the agar surface (Control 1) and then inoculated in another petri dish containing an isolation medium for up to 60 days. Control 2 consisted of the inoculation of water drops from the third rinsing procedure (Teixeira et al. 2019). The seaweed was inoculated, aiming the endophytic fungi to grow, in a medium consisted of potato dextrose agar (39 g/L) prepared in sterile seawater supplemented with 200 mg/L of chloramphenicol (Sarasan et al., 2017). The emerging colony was purified by streaking technique and preserved in flasks containing glycerol or mineral oil, in the Laboratory of Marine Environment Organic Chemistry and at -80°C in

Laboratory of Clinical Mycology, both in School of Pharmaceutical Sciences of Ribeirão Preto, University of São Paulo, Brazil.

Fungal Identification

To the DNA extraction procedures, the isolated fungal strain was cultivated in potato dextrose broth. The identification was carried based on the sequencing of the internal transcribed sequence (ITS) region of the fungal ribosomal DNA. The polymerase chain reactions (PCR) were performed with Phusion® High-Fidelity DNA Polymerase (New England BioLabs, Inc.) and primers ITS1 (5'-T C C GTA GGT GAA CCT GCG G-3') and ITS4 (5'-TCC TCC GCT TAT TGA TAT GC-3') (White et al. 1990). The PCR products were purified with Wizard® SV Gel and PCR Clean-Up System (Promega) and sequenced using the same primers with ABI3730 DNA Analyzer (Applied Biosystems). Each sequence was analyzed with ChromasPro® Software (ChromasPro 1.7.6, Technelysium Pty Ltd., Tewantin QLD, Australia). The sequences were then tested against the publicly available DNA sequences in the National Institutes of Health (NIH) genetic sequence database (Benson et al. 2013).

Fermentation and Extraction

The fungus was grown in Potato Dextrose Agar medium (PDA NEOGEN®, USA, 39 g/L) for 7 days. After this period, 10 plugs (5 mm diameter) were transferred to each of the 50 Erlenmeyer flasks (500 mL), containing 200 mL of Potato Dextrose Broth (PDB KASVI®, BRAZIL, 27 g/L) medium, prepared in artificial seawater SWBG-11 described by Castenholz, 1988. The flasks remained static and at room temperature for 14 days. Liquid-liquid extraction with ethyl acetate was performed to obtain the extracts, adding 100 mL of the solvent in each Erlenmeyer flask followed by 5 minutes in the ultrasonic bath (75 W). The procedure was performed 3 times for each flask. After the method was completed, the aqueous culture medium was properly discarded. The crude extract (CE) was concentrated in a rotary evaporator under reduced pressure and heat, not exceeding the temperature of 28º C.

Crude extract fractionation and compounds isolation

The CE (1.2g) was fractionated by vacuum liquid chromatography (VLC) method, using a stationary phase silica gel (40-70 mesh, Merck) in a 200 mL glass Buchner funnel (18 mm diameter, 250 mm height). Elution using the organic solvents *n*-hexane (Hex), ethyl acetate (EtOAc) and methanol (MeOH) with 200 mL of a stepwise polarity gradient yielded nine fractions: VLC A (Hex 100%), VLC B (Hex:EtOAc 9:1), VLC C (Hex:EtOAc 4:1), VLC D (Hex:EtOAc 3:2), VLC E (Hex:EtOAc 2:3), VLC F (Hex:EtOAc 1:4), VLC G (EtOAc 100%), VLC H (EtOAc:MeOH 7.5:2.5) and VLC I (MeOH 100%). Fractions VLC E and F were selected for compounds isolation after chromatographic analyses and bioguided studies.

Fraction VLC E and F were submitted to purification by reverse phase HPLC (LC-6AD model, Shimadzu) coupled with diode array detector (SPD-M10A model, Shimadzu) with a semi-preparative column C-8 (25cm x 10mm, 10µm - Ascentis Supelco, USA). In this isolation, a polarity gradient method changing concentration of MeOH in distilled water: 15% (0 minutes) - 100% (20 – 22 minutes) - 15% (23 – 25 minutes) was used.

In this way, it was possible to obtain from VLC E the compounds **1**, **3**, and **6**, and from VLC F the compounds **2**, **4**, **5**, and **6**, respectively.

Structure Identification

The isolated compounds were characterized through spectrometry analyses, such as mass spectrometry (MS) and nuclear magnetic resonance (NMR). The MS data were obtained using a spectrometer of Bruker, microTOF Q II with electrospray ionization and analyzer time of flight type (TOF) in Organic Chemistry Laboratory (FCFRP-USP). The NMR spectroscopy was employed to get data from unidimensional (^{1}H) and bidimensional (HMBC, HSQC) analyses. The NMR spectra were acquired in Chemistry Department of Faculty of Philosophy, Sciences and Letters at Ribeirão Preto – USP, using a spectrometer model DRX 500, Bruker, Billerica operating at 500 MHz, using deuterated solvents from Sigma-Aldrich: methanol (CD_3OD), dimethyl sulfoxide (DMSO-d_6) and chloroform ($CDCl_3$). The obtained results were compared with literature data.

Determination of the UV Absorption Spectra

Absorption spectra in the UV region of the CE, fractions and isolated compounds were determined by a spectrophotometer (Agilent 8453) in the 200 to 400 nm range, for the determination of the UV absorption spectra. The samples were diluted in methanol to yield a solution with a concentration of 100 µg/mL. However, the samples that showed higher absorbance in the UVA-UVB region were analyzed in the further studies (photostability, phototoxicity and antioxidant). So, fraction F and the isolated compound **6** were selected to continue our study.

Photostability Test

For the photostability studies, 1 mL of each solution sample was added to glass beakers and then subjected to solvent evaporation until a dried film was obtained. The samples were then submitted or not to UV radiation of 4 mW/cm^2 emitted from a Philips UVA lamp Actinic BL/10 (Eindhoven, Netherlands) (cumulative dose of 27.5 J/cm^2) measured with a Dr. Hönle radiometer (Planegg, Germany) equipped with a UVA sensor. After irradiation, the dried film was resuspended in 1 mL of solvent, and the absorption spectrum of the solutions in the 280 to 400 nm range was analyzed. The area under the curve (AUC), which is the integral of the absorption spectrum of the samples in the UVB (280–320 nm) and UVA (320–400 nm) ranges, were used to calculate the photostability by using the integration function of the MicroCal OriginPro Software (8 SRO, OriginLab Corporation, Northampton, MA, USA). The results of the photostability experiments are expressed as a percentage of the area of irradiated samples related to the area of non-irradiated samples, considered as 100% (Gaspar and Maia Campos, 2006; Tavares et al. 2020).

Toxicity Assessment

Phototoxicity assay (3T3 NRU PT)

The selected fraction (F) and compound **6** (agonodepside B) were submitted to a phototoxicity test based on neutral red (Merck, Darmstadt, Germany) uptake using 3T3 fibroblasts according to Organization for Economic Co-operation and Development (OECD) nº 432 guideline (OECD, 2019). The fibroblasts were cultivated in Dulbecco's modified Eagle medium (DMEM, Carlsbad, CA, USA) supplemented with newborn calf serum (10%, Carlsbad, CA, USA), glutamine (4 mM), penicillin (100 IU/mL) and streptomycin (100 µg/mL) from Sigma Aldrich (St. Louis, MO, USA). In this test 3T3 Balb/c fibroblasts seeded on two 96-well plates (1 x 10^4 cells/well) were pre-incubated with eight different concentrations ranging from 6.81 to 100 µg/mL of the samples analyzed for 1h. Norfloxacin (St. Louis, MO, USA) was used as positive control. One plate was then exposed to a UVA irradiation dose of 9 J/cm^2, using irradiance of 6.8 mW/cm^2 for 22 min obtained with a solar simulator (Dr. Hönle type SOL-500, Planegg, Germany), while another one was kept in the dark. To evaluate the cyto- and phototoxicity of the samples, cell viability in the presence and absence of radiation was determined by the neutral red uptake method. Data were analyzed using Phototox Software 2.0, which calculated the Mean Photo Effect (MPE). According to the phototoxicity determination guideline recommended by OECD (OECD, 2019) sample with MPE < 0.10 predicts "no phototoxicity", while MPE > 0.10 and < 0.15 predict "equivocal phototoxicity"; and MPE > 0.15 predicts "phototoxicity".

Ocular irritation potential (HET-CAM assay)

The Hen's egg test-chorioallantoic membrane (HET CAM) assay was performed according to Luepke and Kemper (1986). Fertilized White Leghorn chicken eggs at the tenth day of incubation at 37 °C under 50–60% relative humidity were used. The eggshell around the air space was removed, the inner membrane was hydrated with a 0.9% NaCl solution and removed carefully, and the chorioallantoic membrane (CAM) was exposed. Three hundred µL of a 0.01% solution (100 µg/mL) of samples (fraction F and compound **6**) were applied to the CAM and 20 seconds after, the CAM was rinsed off with 5 mL of 0.9% NaCl solution and monitored for 5 minutes using a stereo microscope (SZT – Led#, Bel Photonics, Brazil), in order to observe the irritant events such as hyperemia, hemorrhage and coagulation. It was given one score for each observed effect, according to the time of appearance (Table 1). The Irritation Score (IS) was obtained by the sum of individual scores of hyperemia, hemorrhage and coagulation. A sample is classified as non-irritant if $0 \leq IS \leq 0.9$; as slightly irritant if $1.0 \leq IS \leq 4.9$; as moderate irritant if $5.0 \leq IS \leq 8.9$ and as severe irritant if $9.0 \leq IS \leq 21$.

A 1% (w/w) sodium lauryl sulfate (SDS) solution was used as positive control and a 0.9% sodium chloride (NaCl) solution was used as negative control. The test was performed in quadruplicate.

Table 1 Scores given to the irritant events observed in the HET CAM test (adapted from Luepke and Kemper, 1986).

Irritant Event	0 - 30 sec	30 sec – 2 min	2 min – 5 min
Hyperemia	5	3	1
Hemorrhage	7	5	3
Coagulation	9	7	5

Photoprotection against UVA-induced ROS production

HaCat Antioxidant Activity

The quantification of intracellular ROS produced by HaCaT cell exposure to UVA was evaluated using the 2',7'-dichlorodihydrofluorescein diacetate ($DCFH_2$-DA, Sigma Aldrich, St. Louis, MO, USA) probe, a non-fluorescent compound that permeates the cell, is hydrolyzed by intracellular esterases and, oxidized by ROS to the fluorescent compound, 2'-7'-DCF (Kalyanaraman et al., 2011). UVA irradiation provokes ROS generation, which can oxidize DCFH to dichlorofluorescein, a fluorescent product, increasing fluorescence (%).

Prior to the beginning of the assay, cell viability was evaluated to exclude the possibility that the decrease in fluorescence intensity obtained in the ROS assay is related to cell death and not to antioxidant activity. The assay was performed under the same conditions (cell type, density and exposure times) as the measurement of intracellular ROS generation in HaCaT monolayers cells.

Cell viability was evaluated using keratinocytes HaCaT (Cell Bank of Rio de Janeiro, Rio de Janeiro, Brazil), whichwere cultivated in DMEM (Gibco, Carlsbad, CA, USA) supplemented with fetal bovine serum (10%, Gibco, Carlsbad, CA, USA), pyruvate (1 mM), penicillin (100 IU/mL) and streptomycin (100 µg/mL) from Sigma Aldrich (St. Louis, MO, USA). Subsequently, they were seeded in 96-well plates (1×10^5 cells/well) and cultured overnight at 37 °C in a 5% CO_2 atmosphere. The cells were treated with the samples selected for this experiment, fraction F and isolated compound **6**,as it showed the best UV absorbance among the isolated compounds,using concentrations of 10.0; 5.0 and 2.5 µg/mL. The cells were incubated for 1h. Then, cell viability was determined by neutral red uptake (Rangel et al. 2020; Gaspar, Maia Campos and Liebsch, 2013). Sodium dodecyl sulfate (SDS) was used as a positive cytotoxic control (100 µg/mL). The absorbance of untreated cells was considered as 100% to calculate the percentage of cell viability relative to the samples.

For the evaluation of photoprotection against UVA-induced ROS production, HaCaT cells cultivated in supplemented DMEM were seeded in 96-well plates (1×10^5 cells/well) and cultured overnight at 37 °C in a 5% CO_2 atmosphere. The cells were treated and incubated with sample (compound **6** at 10.0; 5.0 and 2.5 µg/mL) for 1h, then they were incubated with $DCFH_2$-DA (10 µM) for 30 min, followed by exposure to UVA radiation (Solar simulator Dr. Hönle type SOL-500, Planegg, Germany) with a total dose of 4 J cm^{-2}, using an irradiance of 6.6 mW/cm for 10 minutes. Quercetin (10 µg/mL) and norfloxacin (100 µg/mL) (Sigma Aldrich, St. Louis, MO, USA) were used as ROS quencher and generator, respectively. The fluorescence was determined with a microplate reader (Synergy™ HT, BioTek, USA) at 485 nm excitation and 528 nm emission. The fluorescence of untreated irradiated cells was considered to be 100% in order to calculate the relative percentage of samples.

Reconstructed Human Skin Model (RHS) Antioxidant Activity

The assay with *in house* reconstructed skin models was conducted after approval by the Ethics Committee in Research Involving Human Beings – School of Pharmaceutical Sciences of Ribeirão Preto – USP (CAAE number 31758619.5.0000.5403), using primary human fibroblasts and keratinocytes from foreskin (pooled from three donors). Informed written consent was obtained from all the donors or their parents or legal guardians.

Primarily, the dermal compartment was prepared by seeding 1.14×10^5 normal human fibroblasts with collagen type I (Corning®) into the insert (0.4 µm pore size; ThinCert™, Greiner Bio-One GmbH, Frickenhausen - Germany) and incubated for 20 hours. After that, 3.7×10^5 normal human keratinocytes were seeded on the top of the dermal compartment and kept submerged in an *in house* prepared culture medium for 24 hours, so the cells could form a monolayer. Throughout 7 days, the culture was maintained at the air-liquid interface allowing complete

keratinocytes differentiation and stratification, and the culture medium was changed every other day (Pennacchi et al, 2015; Pivetta et al, 2019; Tavares et al, 2020).

After the skin models were fully differentiated on day 10, the measurement of intracellular ROS generation began with the incubation of the models with the $DCFH_2$-DA (50 µM) for 45 min in the absence of light. After washing with phosphate-buffered saline (PBS), 25 µL of the **s**ample were applied onto the skin models for 1 hour and then, subjected (UV+) or not (UV-) to 10 $J.cm^{-2}$ of UVA radiation from a SOL-500 solar simulator (Dr Honle AG, Planegg, Alemanha).

Immediately after irradiation and washing with PBS, the tissues were frozen in liquid nitrogen and the, 8 µm histological sections were obtained in a cryostat. Pictures were obtained in an inverted Ti-S microscope (Nikon Instruments Inc., Holland), 488 nm, using 100 ms of exposure intensity and analyzed by Image J software (Marionnet et al., 2014; Rasmussen et al., 2010). Fluorescence intensity results were normalized to area/pixels and expressed as percent fluorescence compared to untreated irradiated (UV+) control.

Statistical analysis

The results were analyzed by one-way ANOVA followed by Tukey's post-hoc test using Minitab version 18.1, since they presented normal distribution (Anderson-Darling test). p-Values lower than 0.05 were considered to be statistically significant.

Results and Discussion

Fungal Identification

The fungal isolate, was obtained from the fragments of *Phaeurus antarcticus* and was later identified as the fungus *Arthrinium* sp. The results of identification process can be observed in Table 2, as well as the NCBI reference and accession number.

Table 2 Results concerning the fungus identification, NCBI reference and accession.

Code	Score	E-value	Identities	Final identification	Reference NCBI Accession	NCBI Accession
LMC8101	937	0.0	98%	*Arthrinium* sp.	JQ411349.1	OR412386

Compound's Identification and Characterization

Six major compounds of fractions VLC E (180.0 mg) and VLC F (141.0 mg) from *Arthrinium* sp. CE was isolated and identified (Fig. 1, **1-6**). The report of compounds **1**, **2** and **6** is unprecedented in species of *Arthrinium*.

Compound **1** (2.0 mg) was obtained as a colorless liquid with λ_{max} 273 and 324 nm. Its molecular formula was established as $C_7H_8O_2$ based on high resolution mass spectrometry (HRMS, ESI), *m/z* 123,0484 $[M-H]^-$. The full structure was determined by ^1H NMR analyses (500 MHz, $CDCl_3$, ppm) by observing chemical shifts (*δ), δ*: 4.66 (2H, *s*, H-7), 6.76 (1H, *dd*, *J*= 7.7, 2.3 Hz, H-6) 6.87 (1H, *br s*, H-2), 6.92 (1H, *d, J*= 7.7 Hz, H-4), 7.23 (1H, *t*, *J*= 7.7 Hz H-5) and ^{13}C NMR (HMBC, HSQC; 500 MHz, CD_3OD, ppm) *δ:* 142.7 (C, C-1), 113.4 (CH, C-2), 157.1 (C, C-3), 114.0

(CH, C-4), 128.8 (CH, C-5), 117.4 (C, C-6), 63.5 (CH_2, C-7). The identity of the compound was confirmed after data comparison with the literature of Alfaro et al., 2003, proving to be 3-Hydroxybenzyl alcohol (Fig. 1, **1**).

Compound **2** (1.0 mg) was obtained as a white powder with [– 0.63° and λ_{max} 244, 238, 277 and 326 nm. Its molecular formula was established as $C_{12}H_{12}O_5$ based on HRMS (ESI), *m/z* 235,0756 $[M-H]^-$. The full structure was determined by ^{1}H NMR analyses (500 MHz, DMSO-*d6*, ppm) *δ*: 1.12 (3H, *d*, *J*= 6.2 Hz, H-11), 2.59 (2H, m, H-9), 3.96 (1H, *m*, H-10), 4.80 (1H, *d*, *J*= 4.9 Hz, OH-10), 6.29 (1H, *d*, *J*= 2.0 Hz, H-5), 6.35 (1H, *d*, *J*= 2.0 Hz, H-7), 6.47 (1H, *s*, H-4), 10.98 (1H, *s*, OH-8). The identity of the compound was confirmed after data comparison with the literature of Gremaud et al., 1994, proving to be 6,8-Dihydroxy-3-[(2R)-2-hydroxypropyl]-1H-2-benzopyran-1-one, also known as (-)-orthosporin (Fig. 1, **2**).

Compound **3** (4.0 mg) was obtained as a light yellow amorphous solid with λ_{max} 241 and 311 nm. Its molecular formula was established as $C_{14}H_{10}O_5$ based on HRMS (ESI), *m/z* 257,0459 $[M-H]^-$. The full structure was determined by ^{1}H NMR analyses (500 MHz, CD_3OD, ppm) *δ*: 2.76 (3H, *s*, H-11), 6.09 (1H, *d*, *J*= 2.0, H-7), 6.21 (1H, *d*, *J*= 2.0, H-5), 6.58 (1H, *br s*, H-2), 6.59 (1H, *br s*, H-4) and ^{13}C NMR (HMBC, HSQC; 500 MHz, CD_3OD, ppm) *δ:* 143.2 (C, C-1), 111.3 (C, C-1a), 115.5 (CH, C-2), 157.1 (C, C-3), 100.1 (CH, C-4), 159.7 (C, C-4a), 96.9 (CH, C-5), 164.2 (C, C-6), 97.4 (CH, C-7), 162.7 (C, C-8), 102.3 (C, C-9a), 164.6 (C, C-10a), 23.1 (CH_3, C-11). The identity of the compound was confirmed after data comparison with the literature of Abdel-Lateff et al., 2002, proving to be 3,6,8-trihydroxy-1-methylxanthone, also known as norlichexanthone (Fig. 1, **3**).

Compound **4** (1.0 mg) was obtained as a yellow amorphous solid with λ_{max} 258 and 327 nm. Its molecular formula was established as $C_{14}H_{10}O_7$ based on HRMS (ESI), m/z 289,0519 $[M-H]^-$. The full structure was determined by ^{1}H NMR analyses (500 MHz, DMSO-*d6*, ppm) δ: 2.58 (3H, *s*, H-11), 6.07 (1H, *d*, *J*= 2.0, H-7), 6.30 (1H, *d*, *J*= 2.0, H-5), 13.61 (1H, *s*, OH-8). The identity of the compound was confirmed after data comparison with the literature of Abdel-Lateff et al., 2002, proving to be 2,3,4,6,8-pentahydroxy-1-methylxanthone, also known as anomalin B (Fig. 1, **4**).

Compound **5** (2.0 mg) was obtained as a light yellow amorphous solid with λ_{max} 239, 254, 313 and 359 nm. Its molecular formula was established as $C_{14}H_{10}O_6$ based on HRMS (ESI), *m/z* 273,0550 $[M-H]^-$. The full structure was determined by ^{1}H NMR analyses (500 MHz, DMSO-*d6*, ppm) *δ*: 2.64 (3H, *s*, H-11), 6.07 (1H, *d*, *J*= 2.0, H-7), 6.22 (1H, *d*, *J*= 2.0, H-5), 6.67 (1H, *s*, H-4), 13.65 (1H, *s*, OH-8). The identity of the compound was confirmed after data comparison with the literature of Abdel-Lateff et al., 2002, proving to be 2,3,6,8-tetrahydroxy-1-methylxanthone, also known as anomalin A (Fig. 1, **5**).

Compound **6** (5.5 mg) was obtained as a strong yellow amorphous solid with λ_{max} 217 and 277 nm. Its molecular formula was established as $C_{24}H_{26}O_7$ based on HRMS (ESI), *m/z* 425.1686 $[M-H]^-$ and fragmentation (MS/MS): *m/z* 425 $[M-H]^-$, 221, 203. The full structure was determined by ^{1}H NMR analyses (500 MHz, $CDCl_3$, ppm) *δ*: 1.66 (3H, *dd*, *J*= 6.8 Hz, 1.0, H-9), 1.79 (3H, *dd*, *J*= 6.8, 1.0 Hz, H-9'), 1.92 (3H, *br d*, *J*= 1.0 Hz, H-10'), 1.97 (3H, *br d*, *J*= 1.0 Hz, H-10), 2.04 (3H, *s*, H-11'), 2.14 (3H, *s*, H-11), 5.36 (1H, *m*, H-8), 5.65 (1H, *m*, H-8'), 6.21 (1H, *s*, H-3), 6.38 (1H, *s*, H-3'), 11.37 (1H, *s*, OH-6), 11.84 (1H, *s*, OH-6') and ^{13}C NMR (HMBC, HSQC; 500 MHz, $CDCl_3$, ppm) *δ:* 102.7 (C, C-1), 146.2 (C, C-2), 104.4 (CH, C-3), 148.6 (C, C-4), 106.8 (C, C-5), 153.2 (C, C-6), 137.2 (C, C-7), 121.4 (CH, C-8), 13.4 (CH_3, C-9), 18.8 (CH_3, C-10), 7.5 (CH_3, C-11), 109.5 (C, C-1'), 144.3 (C, C-2'), 114.0 (CH, C-3'), 146.2

(C, C-4'), 118.3 (C, C-5'), 158.8 (C, C-6'), 137.9 (C, C-7'), 126.1 (CH, C-8'), 13.8 (CH_3, C-9'), 18.5 (CH_3, C-10'), 8.9 (CH_3, C-11'), 162.9 (C, C-12') The identity of the compound was confirmed after data comparison with the literature of Cao et al., 2002, proving to be agonodepside B (Fig. 1, **6**).

Herein, it was possible to characterize compounds from different classes commonly biosynthesized by endophytic fungi, such as xanthones, isocoumarins, and depsides. This demonstrates the metabolic diversity that *Arthrinium* has and its biotechnological and pharmaceutical potential.

Isocoumarins (compound **2**) mainly derived from the polyketide pathways, are abundant in fungi and have several biological activities, such as antifungal, anti-inflammatory, cytotoxic, and antimicrobial (Pal et al., 2011; Saeed, 2016; Noor et al., 2020). Regardless of the metabolic process, most fungal isocoumarins are always characterized by a C-3 carbon substituent, as we can see in the present study for the compound **2** ((-)-orthosporin). According to Song and co-workers (2017), this is the spontaneous outcome of a biosynthetic intramolecular cyclization, which makes the residual polyketide chain a substituent.

Xanthones (compounds **3**-**5**) are natural polyphenolic products. The biosynthetic pathways of these compounds when produced by fungi are distinct from those produced by plants. Birch and Donovan (1953) suggested at first the biogenesis of xanthones production by fungi. Roberts, in 1961, studied this assembly in more detail, through radiolabeled acetate feeding experiments, concluding that polyketides, from malonyl and acetyl CoA, are the precursors of the fungi's xanthones (Badiali et al., 2023). The bioactivity of these compounds depends on the nature and/or positions of their substituents, which makes these structures unique with the possibility of binding to a variety of targets and presenting different biological activities, including antimicrobial, antioxidant, and cytotoxic (El-Seedi et al., 2010; Le Pogam and Boustie, 2016).

Finally, agonodepside B (compound **6**) is a depside that was isolated for the first time from the terrestrial filamentous fungus F7524 (Cao et al., 2002). Depsides are natural products formed by phenolic units, biosynthetically originated from the condensation of orselinic acid and derivatives of orcinol or two units of orselinic acid through the formation of an ester by the polyketide synthase (PKS) itself or by a separate enzyme (Kealey et al., 2021; Legaz et al., 2011).

Determination of the UV Absorption Spectra

The crude extract (CE) (Fig. 2A) and fractions E-I (Fig. 2B) presented a good absorption of the UVA and UVB region indicating the presence of compounds of interest for photoprotective activity. The VLC F (141.0 mg) and VLC G (72.0 mg) fractions presented absorbance in both UVB (280-320 nm), UVA I and II (320-400 nm) ranges. The fractions H (370.0 mg) and I (155 mg) also presented a good absorption in the UVA II and UVB regions, which were lower than VLC F (mainly in the UVA region). The VLC E fraction presented an UVB absorbance lower than those previously mentioned.

The isolated compounds, however, did not show a high absorbance in the UV region when compared to the studied extract and fractions. This result may be due to synergism, which occurs when substances in mixtures show a better biological activity than when isolated. The compound that showed the best absorbance profile in the UVB-UVA range was agonodepside B (**6**, Fig. 3).

The use of this substance as an UV filter should not, however, be discarded. The substance may not exert a potent activity when used alone, but it can be studied to be used in combination with other natural products, or with UV filters already on the market, in order to enhance this effect, as shown in the study by Tavares et al. (2020). In this work, the addition of fucoxanthin in a sunscreen formulation increased its photoprotective potential by 72%. Other studies also show the potential of natural products in association with commercial UV filters, enhancing the SPF and maintaining the safety of sunscreens. As another example, Fernandes and collaborators (2015) studied the association of benzophenone-3 with extracts of an antarctic moss (*Sanionia uncinata*), and found that its aqueous extract significantly increased the SPF of the active compound. In addition, they observed an absence of cytotoxicity (Fernandes et al., 2015; He et al., 2021).

Photostability Studies

The crude extract and the fraction with the highest absorbance in the UVB and UVA I and II regions, as well as agonodepside B (**6**), were submitted to the photostability study. All samples tested in this study were considered photostable, because their UVA and UVB absorption did not present a high reduction after irradiation. These results are shown in Fig. 4 and Table 1.

Table 3 Remaining percentage of the area under the curve of the irradiated samples compared to non-irradiated samples considered as 100% in the UVA and UVB range of the CE, VLC F, and agonodepside B (**6**).

Sample	Remaining percentage of the area under the curve		Stability
	UVA	UVB	
CE	87.92%	92.52%	Photostable
VLC F	103.58%	100.88%	Photostable
Agonodepside B (6)	105.35%	94.27%	Photostable

Some UV filters available in the market present higher photo-instability than the fractions and isolated compound **6** of this study. Rangel and co-workers (2020), studied the photostability of some UV filters on the market and the results showed that benzophenone-3 presented approximately 30% of UV absorption reduction, and the broad-spectrum UV filter avobenzone showed a considerable decrease (about 90% reduction) of UV absorption after exposure to UVA radiation (Rangel et al., 2020; Scarpin et al., 2021).

Photochemical reactions can lead to the degradation of the UV filters and, as a consequence, they can loose their ability to protect against UVB-UVA, considerably decreasing the effectiveness of the sunscreen. In addition, these undesirable photoproducts can cause adverse effects, such as allergy and phototoxicity (Scarpin et al. 2021; Nash and Tanner. 2014). Avobenzone, as example, is known to be photo-unstable, due to the keto-enol tautomerization. The enolic form absorbs in the UVA range, and the diketo form absorbs in the UVC range (Pinto da Silva et al. 2014). Some photoallergic reactions of avobenzone have been studied and correlated with its photodegradation products arylglyoxals and benzyls (Scarpin et al. 2021; Afonso et al. 2014; Karlsson et al., 2009).

Toxicity Assessment

Phototoxicity assay (3T3 NRU PT)

This assay is based on a comparison of the cytotoxicity of a chemical when tested in the presence and in the absence of exposure to a non-cytotoxic dose of simulated solar light (OECD, 2019). The results obtained in this assay are presented in Table 3 and indicate that the control norfloxacin was classified as phototoxic, according to the OECD TG 432, showing an MPE > 0.15, and non-cytotoxic due to IC_{50} (–UV) not detected. Agonodepside B (**6**) and its Fraction F were evaluated at a maximum concentration of 100 µg/mL and were considered non-phototoxic (MPE < 0.10). A negative 3T3 NRU-PT result at sufficiently high concentrations is therefore regarded a sufficient stand-alone indicator for acute photosafety, while a positive result in the 3T3 NRU-PT is always a call for further considerations and probably further testing (Liebsch et al., 2005; Ceridono et al. 2012). However, agonodepside B (**6**) showed values of IC_{50} (–UV) of 17.8 and 12.8 µg/mL and its Fraction F showed values of IC_{50} (–UV) of 7.1 and 6.2 µg/mL, both considered to be cytotoxic in 3T3 NRU PT assay (Fig. 5, Table 3), which may be due to the presence of xanthones, that are known for its cytotoxicity (El-Seedi et al., 2010; Le Pogam and Boustie, 2016; Bedi, et al., 2021).

Table 4 Results of the phototoxicity assay on 3T3 NRU. *IC_{50}* half maximal effective concentration, *(− UV)* non-irradiated, *ND* values not determined.

Sample	Run	MPE	IC_{50} (- UV) µg mL^{-1}	Result
Agonodepside B (6)	1	0.056	17.79	Non-phototoxic/Cytotoxic
	2	0.081	12.84	
Fraction F	1	0.014	7.1	Non-phototoxic/Cytotoxic
	2	0.027	6.2	
Norfloxacin	1	0.526	ND	Phototoxic/Non-cytotoxic
	2	0.511	ND	

Ocular irritation potential (HET-CAM assay)

The HET CAM assay is a useful test for the screening of eye irritation potential of natural compounds, complementing the *in vitro* tests for toxicity (Thiesen et al., 2017; Maia Campos et al., 2019; Rangel et al., 2020). As expected, 0.9% NaCl (negative control) did not cause any irritation event, and 1% SDS solution (positive control) caused hemorrhage on the CAM, with an IS of 12 ± 0 and was classified as a severe irritant. The 0.01% Fraction F solution did not induce any irritant events in CAM during the period of observation, and presented a IS of 0 ± 0, being classified as non-irritant. However, 0.01% Compound **6** was classified as a slight irritant due to hyperemia observed in CAM after application, presenting a IS of 1.5 ± 1.7. The results are shown in Fig 6 and Table 4.

Table 5. IS and classification of the effects of the 0.01% Fraction F and 0.01% Compound 6 from *Arthrinium* sp. in the HET-CAM assay. The 1% SDS and 0.9% NaCl solutions were used as positive and negative controls, respectively.

Sample	Irritation Score	Classification
1% SDS	12 ± 0	Severe Irritant
0.9% NaCl	0 ± 0	Non-irritant
0.01% Fraction F	0 ± 0	Non-irritant
0.01% Compound **6**	1.5 ± 1.7	Slight Irritant

Photoprotection against UVA-induced ROS production

HaCat Antioxidant Activity

Although being considered cytotoxic in 3T3 NRU PT assay, probably due to the higher sensibility of the monolayer model of fibroblast cells (TAVARES et al., 2020), Fraction F maintained the cells viability around 100.03% ± 7.8 in the concentration of 10.0 µg/mL, and its isolated compound, agonodepside B (**6**), proved to be non-cytotoxic for HaCaT cells, with a viability around 97.2% ± 4.7 at the concentration of 10.0 µg/mL. The graph showing the results of the viability test and comparison with untreated cells and cytotoxic control are shown in Fig. 7.

After establishing the safe concentrations to use, the antioxidant potential of Fraction F and agonodepside B (**6**) in HaCaT keratinocytes was assessed by detecting UVA-induced intracellular ROS using $DCFH_2$-DA probe. Quercetin was used as an antioxidant control, resulting in a 71% ± 7.8 decrease in ROS generation, and norfloxacin as a pro-oxidant control, resulting in a 39.5% ± 24.5 increase in ROS production.

According to Fig. 8, Fraction F presented an antioxidant activity statistically equal to quercetin ($p > 0.05$) when tested at 10.0 µg/mL, with a reduction around 66.7% ± 14 in UVA-induced ROS production. On the other hand, lower concentrations of Fraction F, 2.5 and 5.0 µg/mL, did not protect against UVA-induced ROS production ($p > 0.05$) (3.22% ± 3.6 and 10.9% ± 20.9 fluorescence reduction, respectively). The isolated substance agonodepside B (**6**) did not present antioxidant activity in the lowest concentrations, 2.5 and 5.0 µg/mL, resulting in an increase of 6.6% ± 4.5 and 10% ± 2.9 in ROS generation, respectively. However, in a similar manner as Fraction F, at the highest concentration tested (10.0 µg/mL), it was able to protect from intracellular UVA-induced ROS production, with a decrease in the fluorescence of 50.4% ± 5.1, being statistically equal to the positive control quercetin ($p > 0.05$) and different from the untreated control ($p < 0.05$).

The antioxidant activity of the fraction F can be explained by the presence of phenols, polyphenols derivatives, such as those isolated and identified in our research (**2**-**6**). The isolated compound under study agonodepside B (**6**) is also a polyphenolic structure, which also justifies its antioxidant activity similar to quercetin. Phenolic compounds are capable of donating electrons or hydrogen atoms, thereby neutralizing ROS (Souza et al., 2019, Silva et al., 2022). A wide range of antioxidants from marine fungi have been reported, such as the already mentioned phenolic compounds, and also anthraquinones, xanthones, carotenoids, indole derivatives and alkaloids (Vitale et al., 2020). The use of natural fungal and algal products in cosmetic formulations could present advantages when compared to synthetic antioxidants, as they are derived from sustainable sources, maybe not harm the environment, and also being obtained from large-scale fermentation in case of the fungi growth (Vitale et al., 2020).

Reconstructed Human Skin Model (RHS) Antioxidant Activity

Reconstructed human skin models are composed of a differentiated epidermis, with a corneal stratification and a living dermis. Thus, the concentration of 10 µg/mL of compound agonodepside B (**6**) and Fraction F were tested to evaluate the protection against UVA-induced intracellular ROS production in the reconstructed human skin model in order to mimic topical application in a physiologically relevant model that consider skin bioavailability of the tested compounds (Roguet et al., 1994; Afaq et al., 2009; Lee et al., 2017).

According to Fig. 9, the results demonstrated that UVA radiation increased ROS generation in the untreated irradiated reconstructed human skin control (NT +UV) (100%) when compared to the untreated and non-irradiated control (NT -UV), while the vehicle (PBS and ethanol 2%) was not capable of reducing ROS generation, with a fluorescence around 85.7%. The Fraction F and compound (**6**) were able to protect viable epidermis against UVA-induced ROS production, with a reduction of 34.6% and 30.2% in the fluorescence, respectively, both when tested at 10.0 µg/mL. As mentioned, this antioxidant activity can be due to the presence of polyphenolic compounds capable of neutralizing free radicals and other ROS (Souza et al., 2019, Silva et al., 2022), which is in agreement with the protection observed in HaCaT keratinocytes.

Conclusions

The crude extract and fractions F and G from the Antarctic fungus *Arthrinium* sp. showed a good absorption in both UVA I and II and UVB range (280 - 400 nm). From this extract and fractions, six compounds were isolated and characterized, three of them not yet reported in *Arthrinium* species (**1**, **2** and **6**). Among these compounds, agonodepside B (**6**) isolated from fraction E and F showed the best absorbance profile in the UVB-UVA range, and demonstrated to be photostable, non-cytotoxic to HaCaT cells and was classified as a slight irritant in HET-CAM assay; it also did not present any phototoxic potential according to OECD TG 432. Besides that, it was able to protect viable epidermis against UVA-induced ROS production, both in keratinocyte monolayers and in reconstructed human skin models, with a reduction of 30.2% in the fluorescence in 3D skin models. Fraction F presented higher absorption in both UVB (280-320 nm) and UVA I and II (320-400 nm) ranges than agonodepside B (**6**), which can be due to synergism of other compounds present in the fraction. This fraction was also considered photostable, non-cytotoxic to HaCaT cells, non-irritant in HET-CAM assay and not phototoxic. Furthermore, it was also able to protect viable epidermis against UVA-induced ROS production, both in keratinocyte monolayers (effect similar to quercetin) and in reconstructed human skin models. Thus fraction F of Antarctic fungus *Arthrinium* sp presents the best photoprotective potential and has the advantage that it does not need further purifications to obtain the proposed safety and efficacy, however other clinical studies should be performed to confirm its photoprotective and antioxidant potential.

Declarations

Acknowledgements

The authors are thankful to University of São Paulo for providing access to necessary resources, the financial and fellowship support from the Brazilian research funding agencies Coordenação de Aperfeiçoamento de Pessoal de Nível Superior (CAPES) and Conselho Nacional de desenvolvimento Científico e Tecnológico (CNPq). The Department of Biomolecular Sciences and the Núcleo de Pesquisas em Produtos Naturais e Sintéticos – NPPNS are acknowledged.

Funding

This study had financial and logistic support from the Brazilian Antarctic Program PROANTAR/MCTI/CNPq N°64/2013), Brazilian Marine Force, National Institute of Science and Technology (INCT:BioNat), Grant #465637/2014-0, and the State of São Paulo Research Foundation (FAPESP), Grant #2014/50926-0 and 2017/03552-5.

Author contributions

Ana Carolina Jordão: Conceptualization, Methodology, Formal analysis, Investigation, Data Curation, Writing – Original Draft, Review and Editing, Visualization **Gustavo Souza dos Santos, Thaiz Rodrigues Teixeira, Ana Júlia Pasuch Gluzezak, Clarissa Bechuate de Souza Azevedo, Ludmilla Tonani and Karina de Castro Pereira:** Methodology, Formal analysis, Data Curation, Review and Editing **Márcia Regina von Zeska Kress:** Conceptualization,Resources, Supervision **Lorena Rigo Gaspar:** Conceptualization,Resources, Supervision, Review and Editing, Project Administration **Pio Colepicolo:** Resources, Project administration, Funding Acquisition **Hosana Maria Debonsi:** Conceptualization, Resources, Review and Editing,Supervision, Project administration, Funding acquisition.

Ethics Approval

All experimental procedures involving humans were performed in accordance with the principles of the Declaration of Helsinki and were approved by the Human Research Ethics Committee of School of Pharmaceutical Sciences of Ribeirão Preto, São Paulo, Brazil (CAAE number 31758619.5.0000.5403). The written informed consent was signed by all the donors or their parents or legal guardian.

Conflict of Interest

The authors declare no competing interests.

Availability of data and material

The raw data supporting the information of this article will be made available by the authors upon request.

References

1. Abdel-Lateff A, Klemke C, König GM, Wright AD (2003) Two new xanthone derivatives from the algicolous marine fungus *Wardomyces anomalus*. J Nat Prod 66:706-8. https://doi.org/10.1021/np020518b
2. Afaq F, Zaid MA, Khan N, Dreher M, Mukhtar H (2009) Protective effect of pomegranate-derived products on UVB-mediated damage in human reconstituted skin. Exp Dermatol 18:553-61. https://doi.org/10.1111/j.1600-0625.2008.00829.x
3. Afonso S, Horita K, Sousa e Silva JP, Almeida IF, Amaral MH, Lobão PA, Costa PC, Miranda MS, Esteves da Silva JC, Sousa Lobo JM (2014) Photodegradation of avobenzone: stabilization effect of antioxidants. J Photochem Photobiol B 140:36-40. https://doi.org/10.1016/j.jphotobiol.2014.07.004
4. Alfaro C, Urios A, González MC, Moya P, Blanco M (2003) Screening for metabolites from *Penicillium novae-zeelandiae* displaying radical-scavenging activity and oxidative mutagenicity: isolation of gentisyl alcohol. Mutat Res 539:187-94. https://doi.org/10.1016/s1383-5718(03)00166-9

5. Badiali C, Petruccelli V, Brasili E, Pasqua G (2023) Xanthones: Biosynthesis and Trafficking in Plants, Fungi and Lichens. Plants (Basel) 12(4):694. https://doi.org/10.3390/plants12040694
6. Bedi A, Gupta MK, Conlan XA, Cahill DM, Deshmukh SK (2021) Chapter 2 - Endophytic and marine fungi are potential sources of antioxidants. In: Sharma VK, Shah MP, Parmar S, Kumar A Fungi Bio-Prospects in Sustainable Agriculture, Environment and Nano-technology. Academic Press:23-89. https://doi.org/10.1016/B978-0-12-821734-4.00008-3
7. Bedoux G, Hardouin K, Burlot AS, Bourgougnon N (2014) Bioactive components from seaweeds: cosmetic applications and future development. Adv Bot Res 71:345–378. https://doi.org/10.1016/B978-0-12-408062-1.00012-3
8. Benson DA, Cavanaugh M, Clark K, Karsch-Mizrachi I, Lipman DJ, Ostell J, Sayers EW (2013) GenBank. Nucleic Acids Res. 41:D36-424. https://doi.org/10.1093/nar/gks1195
9. Birch AJ; Donovan FW (1953) Studies in relation to biosynthesis. I. Some possible routes to derivatives of orcinol and phloroglucinol. Aust. J. Chem. 6:360–368. https://doi.org/10.1071/CH9530360
10. Cao S, Lee AS, Huang Y, Flotow H, Ng S, Butler MS, Buss AD (2002) Agonodepsides A and B: two new depsides from a filamentous fungus F7524. J Nat Prod. 65:1037-8. https://doi.org/10.1021/np010626i
11. Castenholz RW (1988) [3] Culturing methods for cyanobacteria. Methods in Enzymol 167: 68. https://doi.org/10.1016/0076-6879(88)67004-2
12. Ceridono M, Tellner P, Bauer D, Barroso J, Alépée N, Corvi R, De Smedt A, Fellows MD, Gibbs NK, Heisler E, Jacobs A, Jirova D, Jones D, Kandárová H, Kasper P, Akunda JK, Krul C, Learn D, Wilcox P (2012) The 3T3 neutral red uptake phototoxicity test: practical experience and implications for phototoxicity testing-the report of an ECVAM-EFPIA workshop. Regul Toxicol Pharmacol 63:480–488. https://doi.org/10.1016/j.yrtph.2012.06.001
13. Cordero RR, Feron S, Damiani A, Redondas A, Carrasco J, Sepúlveda E, Jorquera J, Fernandoy F, Llanillo P, Rowe PM, Seckmeyer G (2022) Persistent extreme ultraviolet irradiance in Antarctica despite the ozone recovery onset. Sci Rep 12:1266. https://doi.org/10.1038/s41598-022-05449-8
14. DiNardo JC, Downs CA (2018) Dermatological and environmental toxicological impact of the sunscreen ingredient oxybenzone/benzophenone-3. J Cosmet Dermatol 17:15-19. https://doi.org/10.1111/jocd.12449
15. Ding J, Wu B, Chen L (2022) Application of Marine Microbial Natural Products in Cosmetics. Front Microbiol 13:892505. https://doi.org/10.3389/fmicb.2022.892505
16. El-Seedi HR, El-Barbary MA, El-Ghorab DM, Bohlin L, Borg-Karlson AK, Göransson U, Verpoorte R (2010) Recent insights into the biosynthesis and biological activities of natural xanthones. Curr Med Chem 17:854-901. https://doi.org/10.2174/092986710790712147
17. Fernandes A Da S, Alencar AS, Evangelista H, Mazzei JL, Felzenszwalb I (2015) Photoprotective and toxicological activities of extracts from the Antarctic moss *Sanionia uncinata*. Pharmacogn Mag. 11(41):38-43. https://doi.org/10.4103/0973-1296.149701
18. Fivenson D, Sabzevari N, Qiblawi S, Blitz J, Norton BB, Norton SA (2020) Sunscreens: UV filters to protect us: Part 2-Increasing awareness of UV filters and their potential toxicities to us and our environment. Int J Womens Dermatol 7:45-69. https://doi.org/10.1016/j.ijwd.2020.08.008
19. Gaspar LR, Maia Campos PMBG (2006) Evaluation of the photostability of different UV filter combinations in a sunscreen. Int J Pharm 307:123–128. https://doi.org/10.1016/j.ijpharm.2005.08.029

20. Gaspar LR, Tharmann J, Maia Campos PMBG, Liebsch M (2013) Skin phototoxicity of cosmetic formulations containing photounstable and photostable UV-filters and vitamin a palmitate. Toxicol in Vitro 27:418–425. https://doi.org/10.1016/j.tiv.2012.08.006
21. Greco C, de Mattos-Shipley K, Bailey AM, Mulholland NP, Vincent JL, Willis CL, Cox RJ, Simpson TJ (2019) Structure revision of cryptosporioptides and determination of the genetic basis for dimeric xanthone biosynthesis in fungi. Chem Sci 10:2930-2939. https://doi.org/10.1039/c8sc05126g
22. Gremaud G, Tabacchi R (1994) Isocoumarins of the Fungus *Ceratocystis Fimbriata* coffea, Nat Prod Let 5:2, 95-103. https://doi.org/10.1080/10575639408044041
23. He H, Li A, Li S, Tang J, Li L, Xiong L (2021) Natural components in sunscreens: Topical formulations with sun protection factor (SPF). Biomed Pharmacother. 134:111161. doi: 10.1016/j.biopha.2020.111161
24. Jie F, Liwen H, Zhen S, Wei S, Dong Y, Ya W, Xiaoping M, Zhihua R, Zhicai Z, Guangneng P, Zhijun Z, Junliang D, Suizhong C, Yanchun H (2021) Two metabolites isolated from endophytic fungus *Coniochaeta* sp. F-8 in *Ageratina adenophora* exhibit antioxidative activity and cytotoxicity, Nat Prod Res 35(17):2840-2848. https://doi.org/10.1080/14786419.2019.1675060
25. Kalyanaraman B, Darley-Usmar V, Davies KJ, Dennery PA, Forman HJ, Grisham MB, Mann GE, Moore K, Roberts LJ 2nd, Ischiropoulos H (2012) Measuring reactive oxygen and nitrogen species with fluorescent probes: challenges and limitations. Free Radic Biol Med 52:1-6. https://doi.org/10.1016/j.freeradbiomed.2011.09.030
26. Kealey JT, Craig JP, Barr PJ (2021) Identification of a lichen depside polyketide synthase gene by heterologous expression in Saccharomyces cerevisiae. Metab Eng Commun 13:e00172. https://doi.org/10.1016/j.mec.2021.e00172
27. Karlsson I, Hillerström L, Stenfeldt AL, Mårtensson J, Börje A (2009) Photodegradation of dibenzoylmethanes: potential cause of photocontact allergy to sunscreens. Chem Res Toxicol 22(11):1881-92. https://doi.org/10.1021/tx900284e
28. Thiesen LC, Baccarin T, Fischer-Muller AF, Meyre-Silva C, Couto AG, Bresolin TM, Santin JR (2017) Photochemoprotective effects against UVA and UVB irradiation and photosafety assessment of *Litchi chinensis* leaves extract, J. Photochem. Photobiol. B 167:200–207 https://doi.org/10.1016/j.jphotobiol.2016.12.033
29. Liebsch M, Spielmann H, Pape W, Krul C, Deguercy A, Eskes C (2005) UV-induced effects. Altern Lab Anim. 33:131-146. https://doi.org/10.1177/026119290503301s14
30. Le Pogam P, Boustie J (2016) Xanthones of Lichen Source: A 2016 Update. Molecules 21:294. https://doi.org/10.3390/molecules21030294
31. Lee M, Hwang JH, Lim KM (2017) Alternatives to *In Vivo* Draize Rabbit Eye and Skin Irritation Tests with a Focus on 3D Reconstructed Human Cornea-Like Epithelium and Epidermis Models. Toxicol Res 33:191-203. https://doi.org/10.5487/TR.2017.33.3.191
32. Legaz EM, de Armas R, Vicente C (2011) Bioproduction of depsidones for pharmaceutical purposes. In: Rundfeldt C (ed) Drug development – a case study based insight into modern strategies. In Tech, Rijeka, pp 487-507. https://doi.org/10.4103/2229-4708.72223
33. Li G, Dickschat JS, Guo YW (2020) Diving into the world of marine 2,11-cyclized cembranoids: a summary of new compounds and their biological activities. Nat Prod Rep 37:1367-1383. https://doi.org/10.1039/D0NP00016G

34. Marionnet C, Pierrard C, Golebiewski C, Bernerd F (2014) Diversity of biological effects induced by longwave UVA rays (UVA1) in reconstructed skin. PLoS One 9:e105263. https://doi.org/10.1371/journal.pone.0105263
35. Mitchelmore CL, Burns EE, Conway A, Heyes A, Davies IA (2021) A Critical Review of Organic Ultraviolet Filter Exposure, Hazard, and Risk to Corals. Environ Toxicol Chem 40:967-988. https://doi.org/10.1002/etc.4948
36. Nash JF, Tanner PR Relevance of UV filter/sunscreen product photostability to human safety (2014) Photodermatol Photoimmunol Photomed 30:88-95. https://doi.org/10.1111/phpp.12113
37. Noor AO, Almasri DM, Bagalagel AA, Abdallah HM, Mohamed SGA, Mohamed GA, Ibrahim SRM (2020) Naturally Occurring Isocoumarins Derivatives from Endophytic Fungi: Sources, Isolation, Structural Characterization, Biosynthesis, and Biological Activities. Molecules 25:395. https://doi.org/10.3390/molecules25020395
38. OECD- Organization for Economic Co-operation and Development, OECD guidelines for testing of chemicals test n°. 432: In vitro 3T3 NRU Phototoxicity Test (2019b) Available at: https://doi.org/10.1787/9789264071162-en Accessed: 22 Jun 22
39. Ogaki MB, de Paula MT, Ruas D, Pellizzari FM, García-Laviña CX, Rosa LH (2019). Marine Fungi Associated with Antarctic Macroalgae. In: Castro-Sowinski, S. (eds) The Ecological Role of Micro-organisms in the Antarctic Environment. Springer Polar Sciences. Springer, Cham.
40. Maia Campos PMBG, Benevenuto CG, Calixto LS, Melo MO, Pereira KC, Gaspar LR (2019) Spirulina, *Palmaria Palmata*, *Cichorium Intybus*, and *Medicago Sativa* extracts in cosmetic formulations: an integrated approach of in vitro toxicity and in vivo acceptability studies. Cutan. Ocul. Toxicol. 38:1–25. https://doi.org/10.1080/15569527.2019.1579224
41. Pal S, Chatare V, Pal M (2011) Isocoumarin and its derivatives: an overview on their synthesis and applications. Curr Org Chem 15: 782. https://doi.org/10.2174/138527211794518970
42. Pennacchi PC, de Almeida ME, Gomes OL, Faião-Flores F, de Araújo Crepaldi MC, Dos Santos MF, de Moraes Barros SB, Maria-Engler SS (2015) Glycated Reconstructed Human Skin as a Platform to Study the Pathogenesis of Skin Aging. Tissue Eng Part A 21:2417-25. https://doi.org/10.1089/ten.tea.2015.0009
43. Pinto da Silva L, Ferreira PJ, Duarte DJ, Miranda MS, Esteves da Silva JC (2014) Structural, energetic, and UV-Vis spectral analysis of UVA filter 4-tert-butyl-4'-methoxydibenzoylmethane. J Phys Chem A 118:1511-8. https://doi.org/10.1021/jp4123375
44. Pivetta TP, Silva LBD, Kawakami CM, Araújo MM, Del Lama MPF de M, Naal RMZG, Maria-Engler SS, Gaspar LR, Marcato PD (2019) Topical formulation of quercetin encapsulated in natural lipid nanocarriers: Evaluation of biological properties and phototoxic effect. J Drug Deliv Sci Technol 53:1-11. https://doi.org/10.1016/j.jddst.2019.101148
45. Rangel KC, Villela LZ, Pereira K de C, Colepicolo P, Debonsi HM, Gaspar LR (2020) Assessment of the photoprotective potential and toxicity of Antarctic red macroalgae extracts from *Curdiea racovitzae* and *Iridaea cordata* for cosmetic use. Algal Res 50:1-13. https://doi.org/10.1016/j.algal.2020.101984
46. Rasmussen C, Gratz K, Liebel F, Southall M, Garay M, Bhattacharyya S, Simon N, Vander Zanden M, Van Winkle K, Pirnstill J, Pirnstill S, Comer A, Allen-Hoffmann BL (2010) The StrataTest® human skin model, a consistent in vitro alternative for toxicological testing. Toxicol In Vitro 24:2021-9. https://doi.org/10.1016/j.tiv.2010.07.027
47. Roberts JC (1961) Naturally Occurring Xanthones. Chem. Rev. 61:591–605. https://doi.org/10.1021/cr60214a003

48. Roguet R, Régnier M, Cohen C, Dossou KG, Rougier A (1994) The use of in vitro reconstituted human skin in dermotoxicity testing. Toxicol In Vitro 8:635-9. https://doi.org/10.1016/0887-2333(94)90033-7
49. Rosic NN (2021) Recent advances in the discovery of novel marine natural products and mycosporine-like amino acid UV-absorbing compounds. Appl Microbiol Biotechnol 105(19):7053-7067. https://doi.org/10.1007/s00253-021-11467-9
50. Saeed A (2016) Isocoumarins, miraculous natural products blessed with diverse pharmacological activities. Eur J Med Chem 116:290-317. https://doi.org/10.1016/j.ejmech.2016.03.025
51. Saewan N, Jimtaisong A (2015) Natural products as photoprotection. J Cosmet Dermatol 14:47-63. https://doi.org/10.1111/jocd.12123
52. Sarasan M, Puthumana J, Job N, Han J, Lee JS, Philip R (2017) Marine Algicolous Endophytic Fungi - A Promising Drug Resource of the Era. J Microbiol Biotechnol 27:1039-1052. https://doi.org/10.4014/jmb.1701.01036
53. Scarpin MS, Kawakami CM, Rangel KC, Pereira KC, Benevenuto CG, Gaspar LR (2021) Effects of UV-filter Photostabilizers in the Photostability and Phototoxicity of Vitamin A Palmitate Combined with Avobenzone and Octyl Methoxycinnamate. Photochem Photobiol 97:700-709. https://doi.org/10.1111/php.13407
54. SCCS - Scientific Committee on Consumer Safety, The SCCS notes of guidance for the testing of cosmetic ingredients and their safety evaluation (2018) Available at: https://ec.europa.eu/health/sites/health/files/scientific_committees/consumer_safety/docs/sccs_o_224.pdf Accessed: 22 Jun 22
55. Silva EP, Herminio VL de Q, Motta DN, Soares MBP, Rodrigues L de AP, Viana JD, Freitas FA, Silva APG, Souza F das C do A, Vilas Boas EV de B. (2022) The role of phenolic compounds in metabolism and their antioxidant potential. Res Soc Dev 11(10): 297111031750. https://doi.org/10.33448/rsd-v11i10.31750
56. Souza EL, Albuquerque TMR, Santos AS, Massa NML, De Alves JLB (2019) Potential interactions among phenolic compounds and probiotics for mutual boosting of their health-promoting properties and food functionalities – a review. Crit Rev Food Sci Nutr 59(10):1-15. https://doi.org/10.1080/10408398.2018.1425285
57. Sureram S, Kesornpun C, Mahidol C, Ruchirawat S, Kittakoop P (2013) Directed biosynthesis through biohalogenation of secondary metabolites of the marine-derived fungus *Aspergillus unguis* RSC Adv. 3(6):1781-1788 https://doi.org/10.1039/C2RA23021F
58. Tavares RSN, Kawakami CM, Pereira KC, do Amaral GT, Benevenuto CG, Maria-Engler SS, Colepicolo P, Debonsi HM, Gaspar LR (2020) Fucoxanthin for Topical Administration, a Phototoxic vs. Photoprotective Potential in a Tiered Strategy Assessed by In Vitro Methods. Antioxidants (Basel) 9:328. https://doi.org/10.3390/antiox9040328
59. Tavares RSN, Maria-Engler SS, Colepicolo P, Debonsi HM, Schäfer-Korting M, Marx U, Gaspar LR, Zoschke C (2020) Skin Irritation Testing beyond Tissue Viability: Fucoxanthin Effects on Inflammation, Homeostasis, and Metabolism. Pharmaceutics 12:136. https://doi.org/10.3390/pharmaceutics12020136
60. Teixeira TR, dos Santos GS, Turatti ICC, Paziani MH, Kress MR von Z, Colepicolo P, Debonsi HM (2019) Characterization of the lipid profile of Antarctic brown seaweeds and their endophytic fungi by gas chromatography–mass spectrometry (GC–MS). Polar Biol 42:1431-1444. https://doi.org/10.1007/s00300-019-02529-w

61. Teixeira TR, Rangel KC, Tavares RSN, Kawakami CM, dos Santos GS, Maria-Engler SS, Colepicolo P, Gaspar LR, Debonsi HM (2021) In vitro evaluation of the photoprotective potential of quinolinic alkaloids isolated from the Antarctic marine fungus *Penicillium echinulatum* for topical use. Mar Biotechnol 23:357–372. https://doi.org/10.1007/s10126-021-10030-x
62. Thiesen LC, Baccarin T, Fischer-Muller AF, Meyre-Silva C, Couto AG, Bresolin TMB, Santin JR (2017) Photochemoprotective effects against UVA and UVB irradiation and photosafety assessment of *Litchi chinensis* leaves extract. J Photochem Photobiol B 167: 200-207. https://doi.org/10.1016/j.jphotobiol.2016.12.033
63. Vitale GA, Coppola D, Palma Esposito F, Buonocore C, Ausuri J, Tortorella E, de Pascale D (2020) Antioxidant Molecules from Marine Fungi: Methodologies and Perspectives. Antioxidants (Basel) 9(12):1183. https://doi.org/10.3390/antiox9121183
64. Watkins YSD, Sallach JB (2021) Investigating the exposure and impact of chemical UV filters on coral reef ecosystems: Review and research gap prioritization. Integr Environ Assess Manag 17:967-981. https://doi.org/10.1002/ieam.4411
65. White TJ, Bruns TD, Lee SB, Taylor JW (1990) Amplification and Direct Sequencing of Fungal Ribosomal RNA Genes for Phylogenetics. In: Innis MA, Gelfand DH, Sninsky JJ, White TJ. PCR Protocols: A Guide to Methods and Applications. Academic Press 315-322. http://dx.doi.org/10.1016/B978-0-12-372180-8.50042-1
66. Zhang Y, Shah P, Wu F, Liu P, You J, Goss G (2021) Potentiation of lethal and sub-lethal effects of benzophenone and oxybenzone by UV light in zebrafish embryos. Aquat Toxicol 235:105835. https://doi.org/10.1016/j.aquatox.2021.105835

Figures

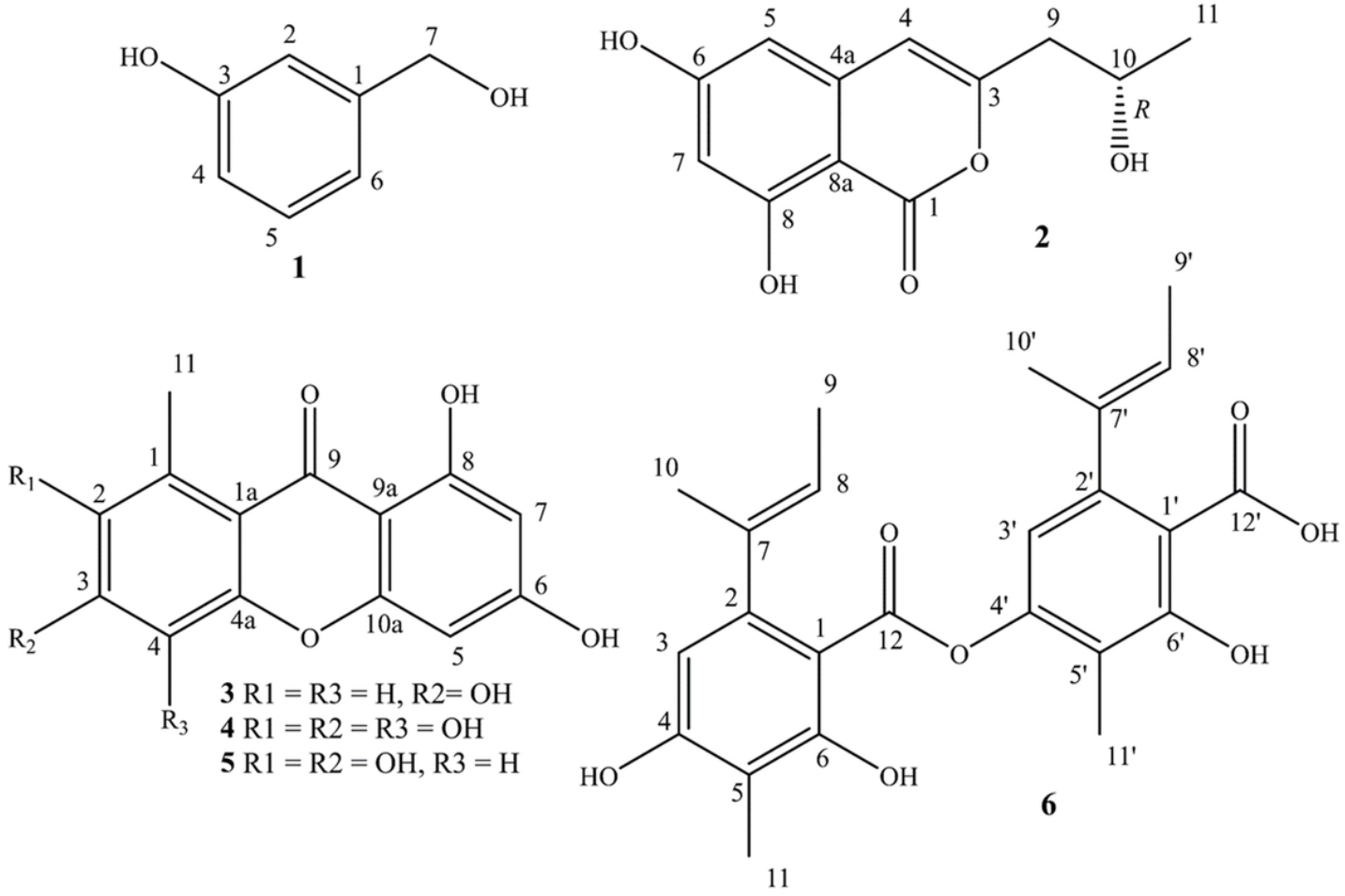

Figure 1

Major compounds isolated from antarctic *Arthrinium* sp. extract.

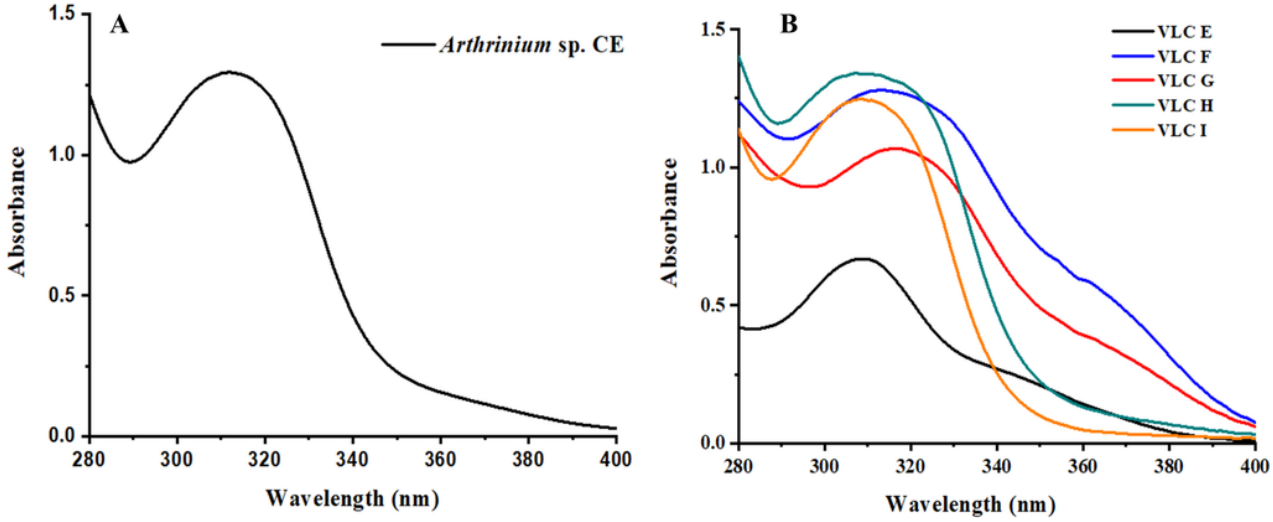

Figure 2

Absorption spectra of the crude extract (CE) (A) from *Arthrinium* sp. fungus and the obtained fractions (B).

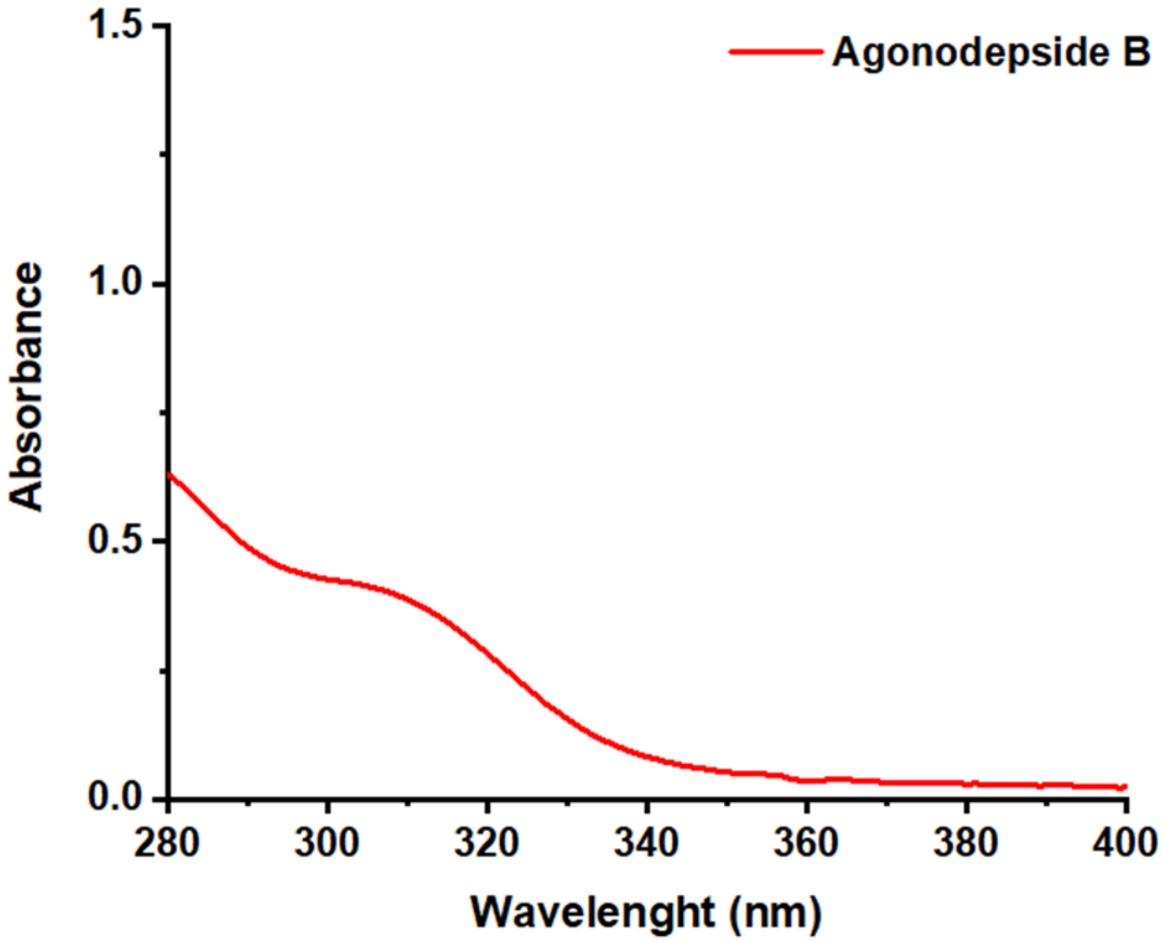

Figure 3

Absorption spectra of agonodepside B (**6**) in the UVB-UVA range.

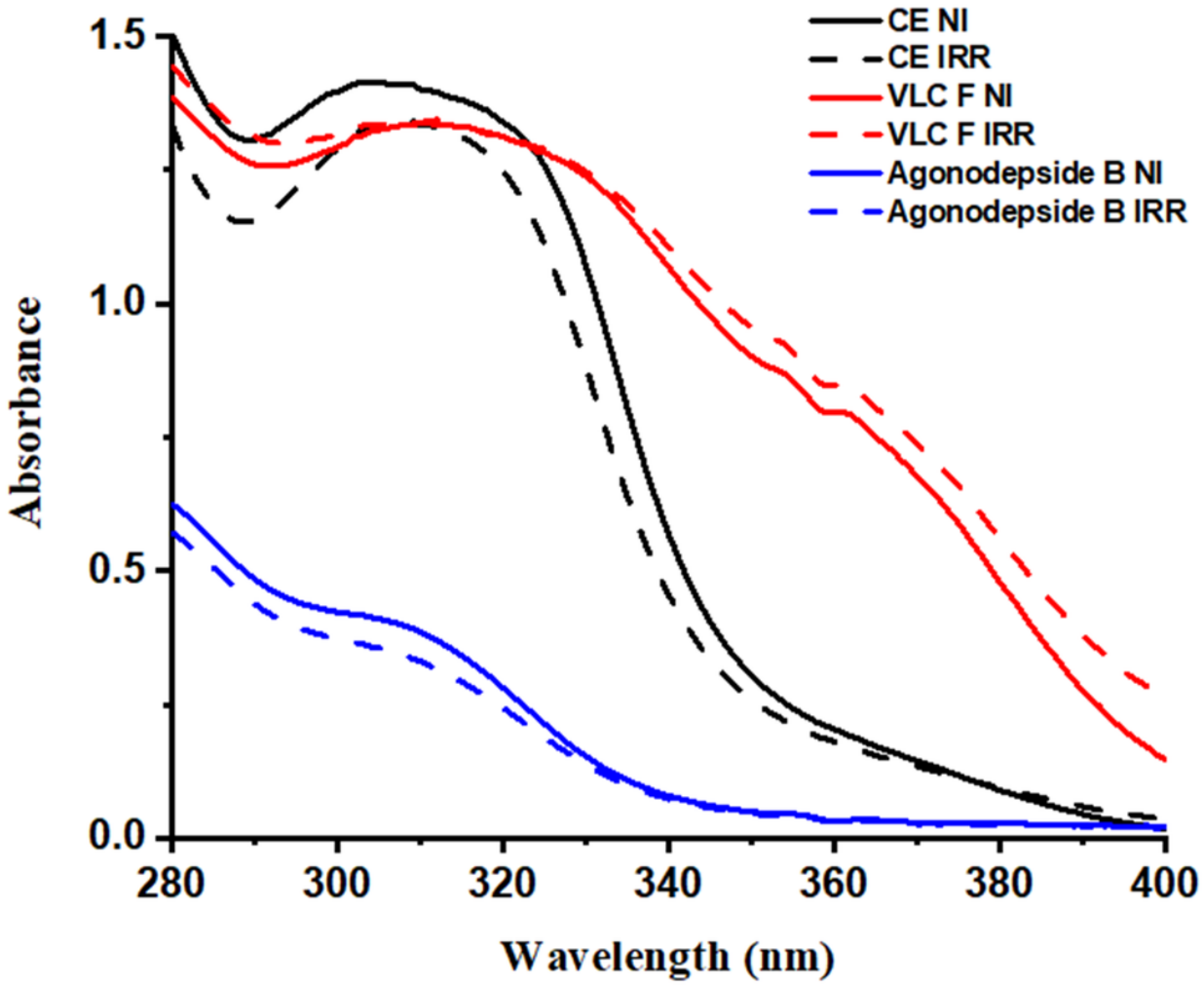

Figure 4

Absorption spectra of the CE, VLC F fraction and agonodepside B (**6**), irradiated (IRR) and non-irradiated (NI).

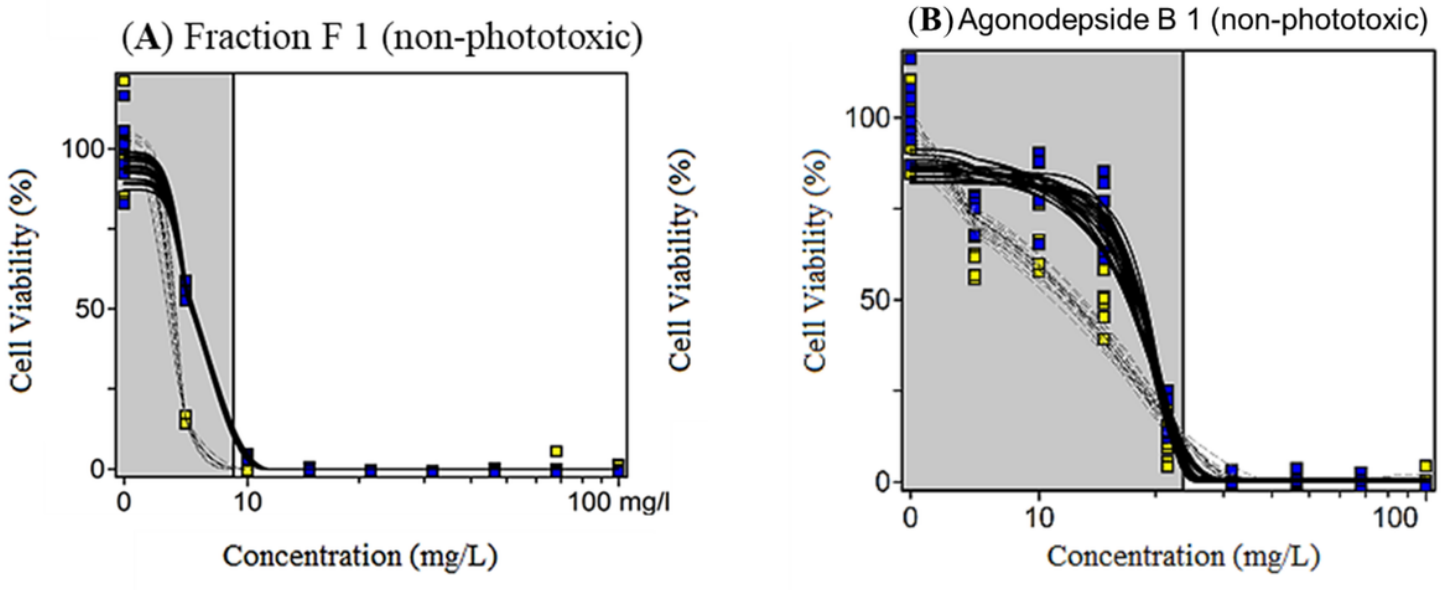

Figure 5

The dose–response curves of fraction F (A) and agonodepside B (**6**) (B) obtained by the 3T3 NRU phototoxicity test and plotted using the Phototox 2.0 software program. The blue and yellow dots refer, respectively, to non-irradiated cells (-UV) and irradiated ones (+UV). Evaluated doses: 6.81, 10, 14.7, 21.4, 31.6, 46.4, 68.1 and 100 $\mu g.mL^{-1}$.

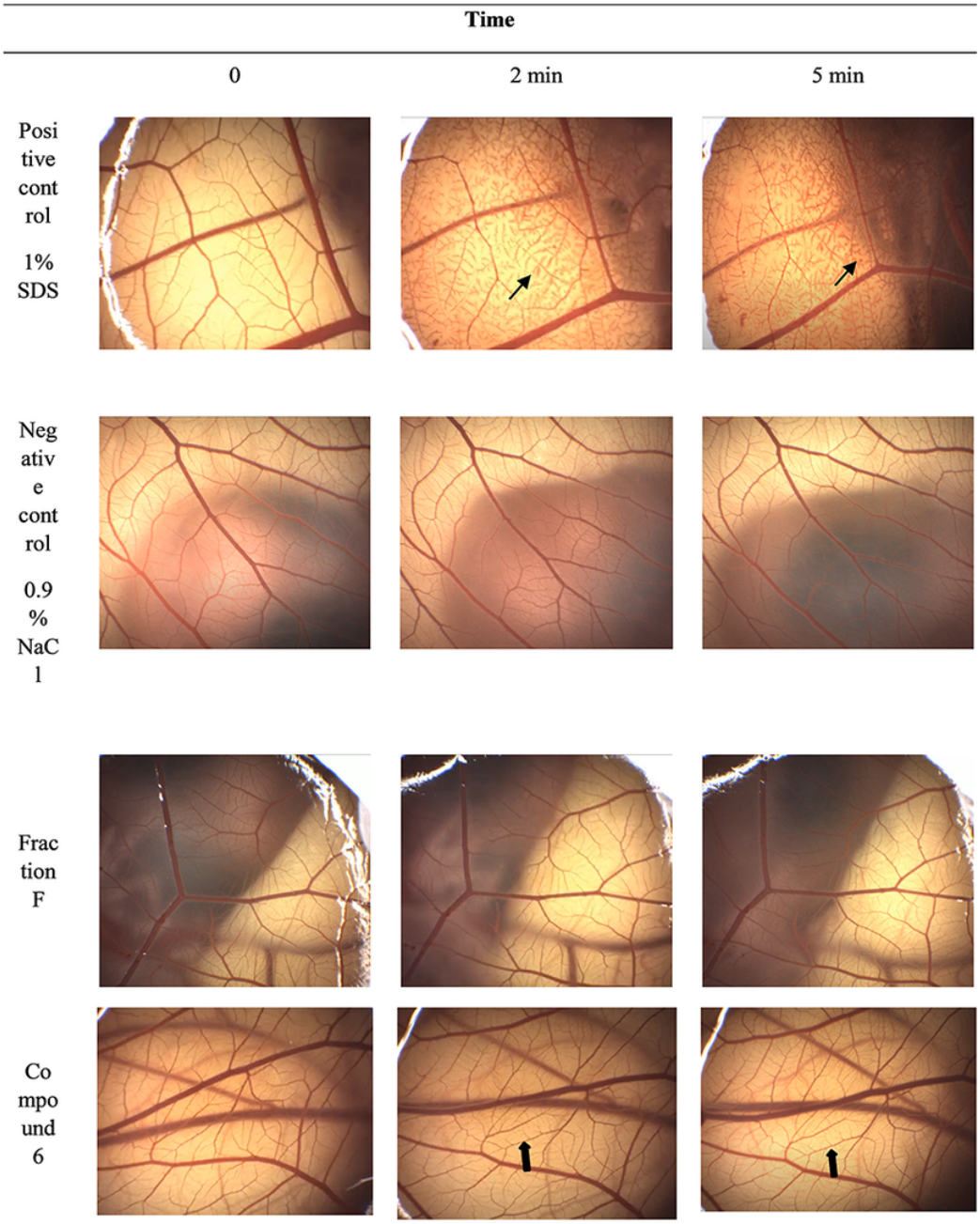

Fig. 6 Evaluation of the irritant potential of 0.01% Fraction F and 0.01% Compound **6** by the HET-CAM assay. The ⬆ indicates hyperemia and ↑ indicates hemorrhage.

Figure 6

See image above for figure legend

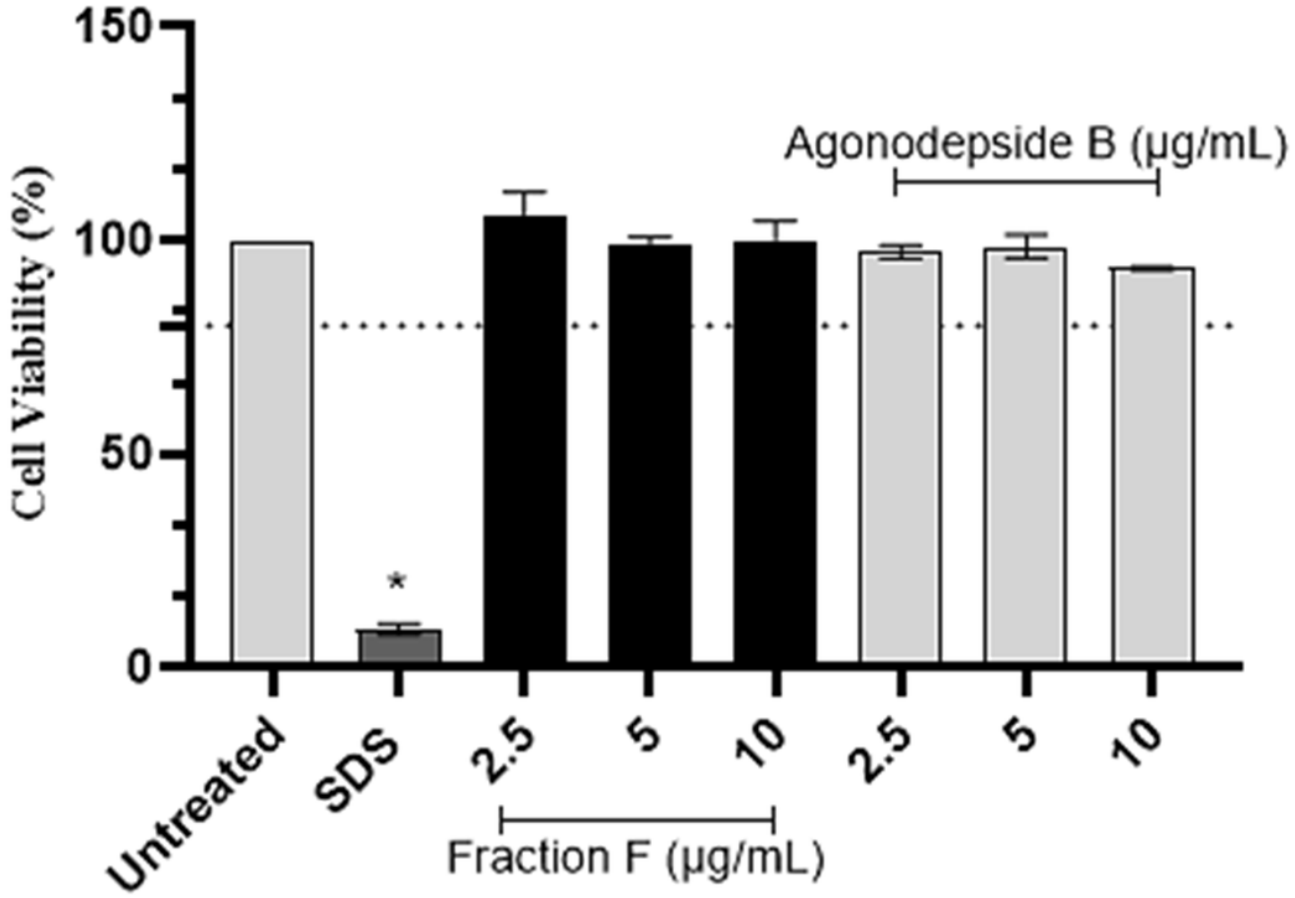

Figure 7

Cell viability (%) of Fraction F and agonodepside B (**6**) at different concentrations. The results are expressed as mean ± standard errors of the mean of three independent experiments (n = 3). Where “*” means statistically different from untreated control ($p < 0.05$).

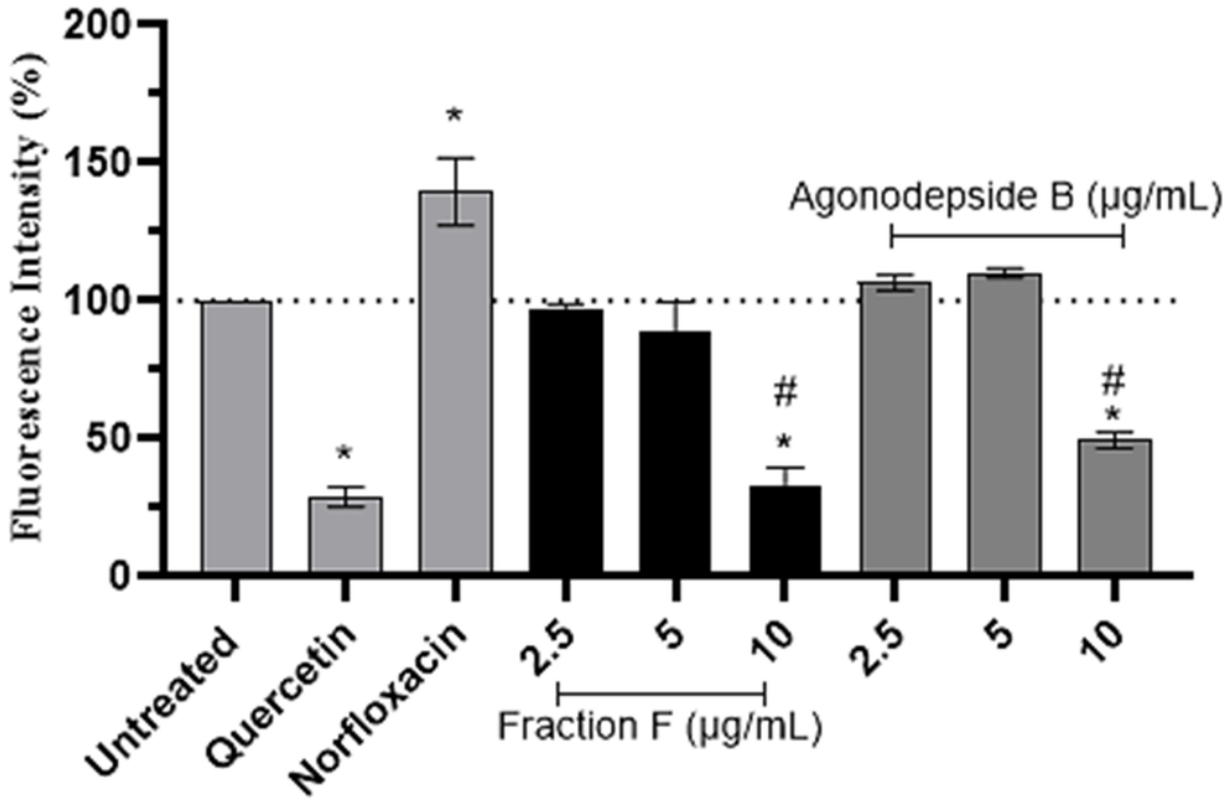

Figure 8

Effects of the pretreatment of HaCaT cells for a period of 24 h on ROS generation induced by UVA irradiation (4 J/cm^2). The results are expressed as % fluorescence. The cells were pretreated with: quercetin (10 µg/mL), norfloxacin (100 µg/mL); Untreated irradiated control (100% fluorescence); Fraction F (2.5, 5, 10 µg/mL); Agonodepside B (2.5, 5, 10 µg/mL). The results are expressed as mean ± standard errors of the mean of three independent experiments (n = 3). Where "*" means statistically different from untreated irradiated control ($p < 0.05$), and "#" means statistically equal to quercetin ($p > 0.05$).

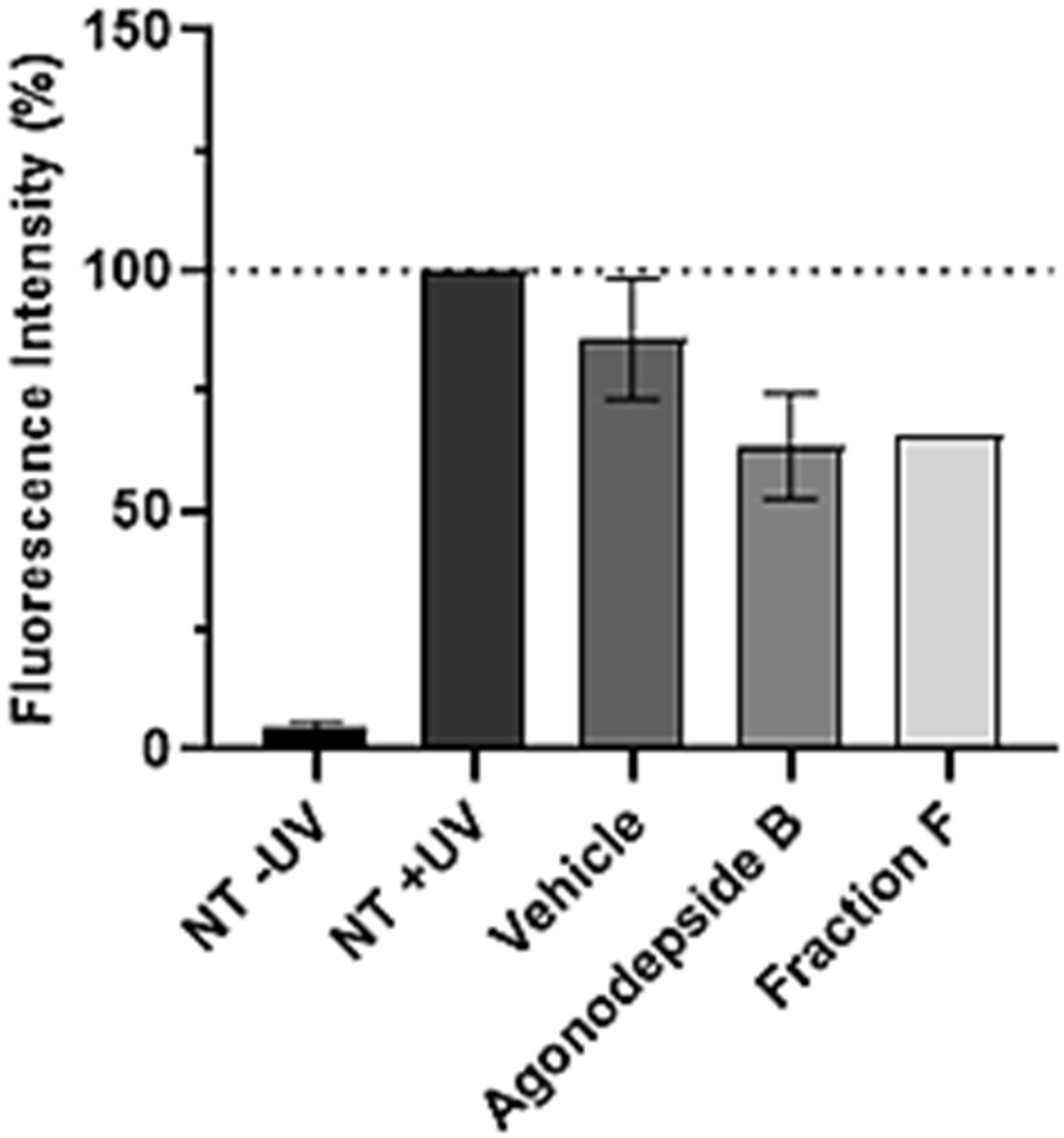

Figure 9

Protection against UVA-induced intracellular ROS production in reconstructed human skin model treated with agonodepside B (**6**) and Fraction F (10.0 µg/mL) and the vehicle PBS with ethanol 2%. NT +UV: irradiated non-treated control; NT -UV: non-irradiated non-treated control.

Supplementary Files

This is a list of supplementary files associated with this preprint. Click to download.

- Supplementaryinformation.docx